CHEMICAL ENGINEERING TRANSACTIONS
VOL. 28, 2012
A publication of AIDIC
The Italian Association of Chemical Engineering
Online at: www.aidic.it/cet
Guest Editor: Carlo Merli
Copyright © 2012, AIDIC Servizi S.r.l.,
ISBN 978-88-95608-19-8; **ISSN** 1974-9791
DOI: 10.3303/CET1228021

Transport Characteristics of Green-Tea Nano-scale Zero Valent Iron as a Function of Soil Mineralogy

Maria Chrysochoou*[a], Meghan McGuire[a], Geeta Dahal[b]

[a]Department of Civil and Environmental Engineering, University of Connecticut, Storrs, CT, 06269, USA.
[b] VeruTEK Inc., Bloomfield, CT, 06002, USA
mchrysoc@engr.uconn.edu

The transport characteristics of iron nanoparticles prepared with a green tea, polyphenol-rich solution, were investigated for two granular media, pure silica sand and sand coated with aluminium hydroxide. The GT-nZVI injection caused a sharp decrease in the effluent pH and increase in the redox potential, which is attributed to the presence of free Fe^{3+} and polyphenols in the suspension, respectively. The breakthrough curves for total Fe in the outflow indicated that some aggregation and deposition of nanoparticles occurred in both types of sand. However, the majority of the iron mass was detected in the outflow (73 % in the uncoated and 62 % in the coated sand), indicating good transport of the nanoparticles. XRF results indicated that no iron was retained on the Al-coated sand particles, while 4 % of the injected Fe was deposited on the pure silica particles. This behaviour is attributed to the electrostatic interactions between the positively charged nanoparticles and the positively charged Al-coatings vs. negatively charged silica in the pH range of the experiments. The “missing” iron in the Al-coated sand columns was observed as a reddish brown precipitate in the 0.7 μm filter that was placed in the outflow of the columns; thus, increased agglomeration was observed compared to the pure silica sand columns. This study shows that soil geochemistry can have a significant effect on the transport characteristics of nanoparticles in porous media.

1. Introduction

An established approach in contaminant removal is the utilization of zero valent iron (ZVI) mediated remediation that exploits iron corrosion chemistry to subsequently form solid iron precipitation resulting in immobilization of contaminants. ZVI is iron in zero oxidation state with incompletely filled d-orbitals. ZVI thus has the potential to readily loose electrons making it very reactive. Remedial approaches involving the use of ZVI to treat various halogenated organic compounds and heavy metals in soil and groundwater have gained popularity in the recent years (Li et. al, 2006). The particle size of ZVI is commonly in the mm to cm scale, and one application limitation is the difficulty to inject ZVI in the subsurface; instead, it is commonly used to construct permeable reactive barriers. A recent innovation in the use of zero oxidation state iron is the diminution of ZVI particles to nano-sized particle, commonly referred to as nanoscale zero-valent iron (nZVI). The nano-scale size of nZVI implies larger surface area to volume ratio which results in enhanced reactivity (Hoag et al., 2009), and the potential to form an injectable suspension. Injection of nZVI into the subsurface could potentially be a promising alternative to ZVI permeable reactive barrier. The smaller size of nZVI provides application flexibility PRBs as nanoparticles can be transported through porous media (Elliott and Zhang, 2001).
While the enhanced reactivity of the iron nanoparticles could lead to passivation effects via oxidative loss, nZVI agglomeration influenced by the magnetic properties of iron (Phenrat et al., 2009) also result

Please cite this article as: Chrysochoou M., Mcguire M. and Dahal G., 2012, Transport characteristics of green-tea nano-scale zero valent iron as a function of soil mineralogy, Chemical Engineering Transactions, 28, 121-126 DOI: 10.3303/CET1228021

in transport-related disadvantages. In addition, reduction of hexavalent chromium (Cr(VI)) by ZVI is thought to be a surface-mediated process, where Cr(VI) is adsorbed onto the iron surface and subsequently reduced (Cao and Zhang, 2006); agglomeration of the nZVI particles implies that the available surface area for reaction is reduced as a result of coagulation. Agglomeration thus inhibits both nZVI reactivity and mobility. Various coatings, emulsions and stabilizing agents have been used to create stable nanoparticle suspensions in order to deter agglomeration and prevent passivation. (Franco et al., 2009) An innovative approach to nZVI stabilization has used an extract of green tea that contains polyphenols as the coating ingredient (Hoag et al., 2009).

Studies on nanoparticle transport in porous media have primarily employed pure silica sands to investigate effects such as the type of coatings, size and concentration of nanoparticles (example of such studies include Kanel and Choi, 2007 and Phenrat et al., 2009). There is little information on the effect of geochemical parameters, such as pH and soil mineralogy on the transport characteristics of iron nanoparticles. Recently, Kim et al. (2012) found that decreasing pH caused increased agglomeration of nVI particles covered with polyelectrolytes and that the presence of kaolinite particles in the soil also caused increased agglomeration compared to smaller size silica particles. The surface charge of different types of surfaces can result in different types of interaction with the nanoparticles, which is also a function of pH. This study explores the transport characteristics of nanoscale green tea zero valent iron (GT-nZVI) with pure sand and sand coated with Al-hydroxide.

2. Materials and Methods

2.1 Preparation of sands and reagents

Ottawa sand (flint silica #13) with an average particle size of 480 μm was used for all experiments. The aluminium coated sand was prepared according to the procedure described in Chen et al. (1998). All chemicals used were analytical grade (Fisher Scientific, Pittsburgh, PA). 1000 g of sand was rinsed with water until it ran clear. Then the sand was mixed with a 1.0 M $AlCl_3$ solution for 30 min, drained and air-dried. The resulting solid was mixed with 1000 mL of 3.0 M NH_4OH for 10 min, drained and air-dried, then rinsed with DI water and air-dried again. The resulting Al concentration on the sand was determined by acid digestion and Inductive Coupled Plasma (ICP) analysis to be 532 mg/kg.

The GT-nZVI solution was prepared according to Hoag et al (2009). A 20 g/L green tea solution was brewed by bringing water mixed with green tea leaves to 80 °C. The solution was then mixed with a 0.1 M $FeCl_3$ solution at 1:2 volumetric ratio. This yielded a final solution with 66 mM total Fe concentration, at least 65 % of which is estimated to consist of iron nanoparticles (Chrysochoou et al., 2012).

The electrolyte solution for the remaining of the column experiments was a 10 mM Na^+ solution prepared according to Phenrat et al. (2009) by mixing equal volumes of 10 mM NaCl and $NaHCO_3$ solutions with a final pH of approximately 8.5.

2.2 Column studies

Soil columns were made of clear acrylic tubes with an inner diameter of 3.4 cm and length 17.5 cm. Approximately 280 g were packed manually in five layers in each column, with a target dry density of 1.7 g/cm^3. The resulting pore volume (PV) was 53 mL. Four columns were set up, two containing pure silica sand and two with Al-coated sand.

Influent was injected into the columns at a rate of 1 mL/min using a Manostat Carter cassette pump. All columns were flushed with 2 PV of electrolyte solution, followed by one PV of GT-nZVI and 5 PV of electrolyte solution, until the Fe concentration in the outflow was reduced to background concentration (5 mg/L) for three consecutive PVs. Sampling of the outflow was performed every PV before and every third of a PV (17 mL) after the injection of the GT-nZVI, in order to capture the large fluctuations in the measured parameters following injection.

The pH and redox potential (ORP) in the outflow were monitored using InLab Pro pH and redox electrodes (Mettler-Toledo, Columbus, OH), respectively. Total Fe concentrations were analyzed using a 3000 Series Atomic Absorption Spectrometer (Thermo Scientific, Waltham, MA) according to methods EPA 7010 (graphite furnace) and EPA 7000B (flame). Spectrometer calibration and drift were monitored periodically using blank, spiked, and duplicate samples. After the completion of the experiments, the columns were disassembled and the soil was collected in five layers. Soil pH analysis

was conducted according to method ASTM D4980-89. Total Fe in the soil was measured before and after the tests using an InnovX portable X-ray Fluorescence (XRF) instrument, according to EPA method 6200.

3. Results and Discussion

The pH, redox potential, total Fe in the outflow and normalized breakthrough curves are shown in Figure 1. The pH in the Al-coated sand column effluent during the first PV was 4, possibly due to washing off of excess Al^{3+} from the sand, which can consume OH^- through hydrolysis. The pH quickly increased to neutral by PV 2, after which the GT-nZVI solution was injected.

All columns exhibited an immediate decrease in effluent pH to approximately 2 upon injection, which is attributed to the acidic pH of the GT-nZVI solution. While most nZVI suspensions typically have pH around 9, which is the pH of the ZVI corrosion products (Reardon, 2005), the GT-nZVI pH is stable at 1.5, regardless of exposure to oxygen and progressive corrosion. Because GT-nZVI is made using a $FeCl_3$ solution, it is believed that unreacted Fe^{3+} is responsible for this behaviour (Chrysochoou et al., 2012). The pH remained at 2 from PV 3 to PV 4.3, after which it progressively rebounded to the influent solution pH of 8.5. The pH rebound occurred slightly faster in column Al-sand-2, but there was no difference between the two pure sand columns and Al-sand-1. At pH 2, $Al(OH)_3$ becomes soluble and it conceivable that its dissolution can buffer the pH faster compared to a pure silica sand, that has no buffering capacity; however, this phenomenon was not observed, potentially because the imparted acidity was much higher than the contribution of the buffering reactions. In 53 mL GT-nZVI solution, there are 3.5 mmol of total Fe; if 1 mmoL is present as Fe^{3+}, then its complete hydrolysis to $Fe(OH)_3$ can produce 6 mmol H^+ for 280 g soil or 21 mmol H^+/kg soil, which is a very large amount of acidity.

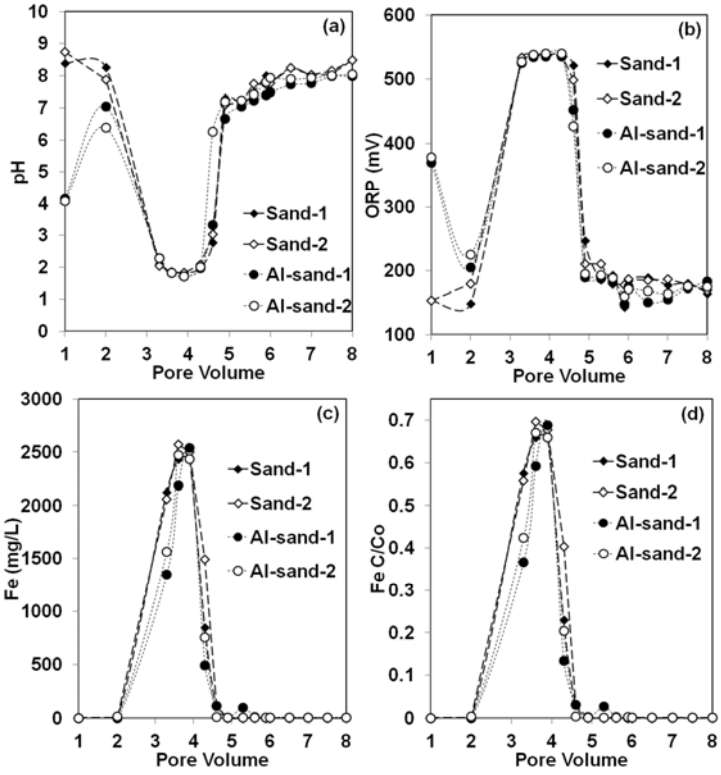

Figure 1: pH (a), redox potential (b), total Fe concentration (c) and Fe breakthrough curve (d) in the outflow of the pure sand and Al-coated sand columns

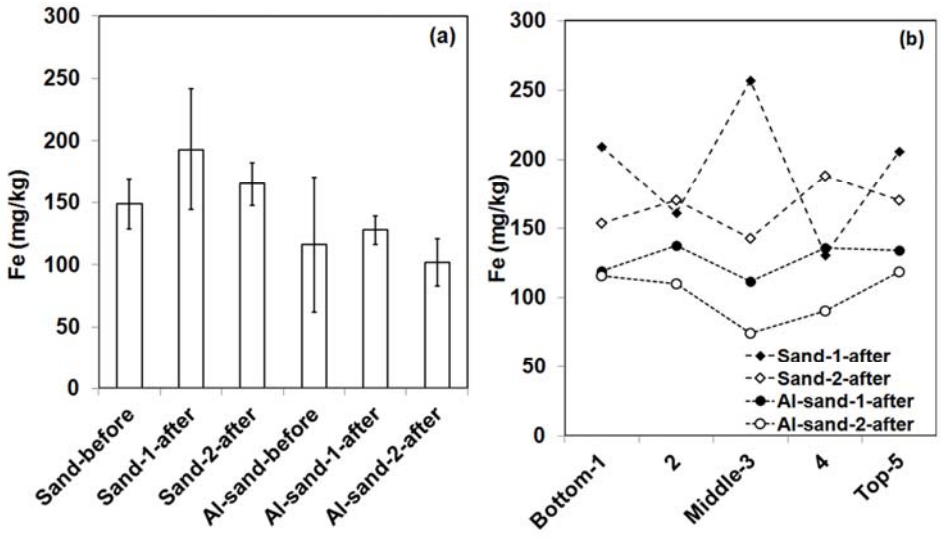

Figure 2: Average Fe concentration in the column sands before and after the GT-nZVI experiments (a), and average Fe concentration in individual layers of the treated columns after the experiments (b).

The GT-nZVI also exhibited different properties compared to conventional nZVI with regard to the redox potential. The redox potential of the GT-nZVI solution is highly oxidizing, approximately 550 mV, despite the fact that it has proven reductive capacity (Chrysochoou et al., 2012). While there is no clear evidence to explain this phenomenon, the authors attribute this property to the presence of high concentration of polyphenols in the mixture, which may oxidize readily and functions as protective anti-oxidants for the nanoparticles. As a result, the redox potential in the column effluent increased from 150 to 550 mV upon injection, and progressively returned to background values by PV 5. Redox potential is often used in the field as an indicator of reducing conditions, which in turn signal the presence of the injected reductant in the subsurface and can be used to assess the radius of influence of a given injection point. Given the very high redox potential of GT-nZVI, it is conceivable that the redox potential may still be used as an indicator of the presence of GT-nZVI solution in the subsurface, using high instead of low redox potentials as the criterion. Accordingly, GT-nZVI appears to have been washed out simultaneously from all four columns in this study, with no apparent difference between pure and Al-coated sand.

The Fe concentration and normalized breakthrough curves (Figure 1c and 1d) presented some differences for the two column types, which is related to the different interaction between the silica and alumina surfaces with the nanoparticles. While the peak concentration of Fe was the same in both columns, approximately 2,500 mg/L, the two Al columns had a slower onset of Fe breakthrough and an overall narrower bell curve, indicating that the total mass of Fe that exited the Al-coated-sand columns was less. The breakthrough curve indicated that the maximum Fe concentration was at C/C0=0.7, whereby C=3.7 g/L. Phenrat et al. (2009) showed normalized breakthrough curves for polymer-modified nZVI as a function of particle concentration and iron content. The maximum C/C0 ratio at 3 g/L particle concentration was ~0.65 for a Fe^0 content of 63 % and 0.85 for a Fe^0 content of 9 %. It follows that the GT-nZVI behaviour, with slightly higher particle concentration of 3.7 g/L, potentially resembles the material with 63 % Fe^0 content. The reduction in the Fe^0 maximum in the normalized breakthrough curve is a result of the aggregation and deposition of the particles on the sand grains (Phenrat et al., 2009). This was further investigated by measuring the Fe content of the sand in the columns before and after the experiments. Ten measurements were performed for the untreated sand prior to the test and ten measurements in each column after the test, divided in five vertical layers.

The average concentration of iron in the untreated sand was 150 mg/kg on average in the pure sand and 115 mg/kg in the Al-coated sand, even though the differences between them were not statistically significant. It is, however, possible, that processing the sand with chemicals for Al-coating removed

some of the existing iron on the particle surfaces. The iron concentration on the pure sand after the injection was slightly higher (180 mg/kg on average) and statistically significant at the 90 % confidence interval ($p<0.1$), whereby measurements of the bulk sand prior to filling up the columns were compared with all measurements from both columns after the completion of the experiments. This was done because the sand tested by XRF before the test was distributed to both columns for testing, so that the sample source and size was comparable for the statistical analysis. The average concentration in the Al-coated columns remained at 115 mg/kg considering both columns and there was no statistical significance between the two groups of measurements before and after the test ($p=0.98$). Thus, the Al-coated columns showed no interaction between the sand particles and the iron nanoparticles, while the pure sand particles indicated a small accumulation of Fe on their surface. This was a surprising result, given the observations in the breakthrough curves and geochemical considerations. The Fe concentrations in the sand were relatively evenly distributed with height in all columns (Figure 2b), indicating good transport of the nanoparticles as well. A mass balance on Fe was conducted in order to further elucidate this behaviour, shown in Table 1.

Table 1: Mass balance for Fe in the columns before and after the experiments

	Fe in sand before (mg)	Fe in GT-nZVI (mg)	Fe in outflow (mg)	Fe in sand after (mg)	Difference In-Out (mg)	% Difference
Sand-1	44	197	138	57	59	24
Sand-2	42	197	150	46	48	20
Al-sand-1	32	197	118	36	80	35
Al-sand-2	32	197	126	29	71	31

The mass in the sand before and after was calculated by multiplying the average XRF concentration with the mass of soil in each column, the amount of Fe in the injected GT-nZVI was calculated as 56 mM* 53 mL of injected volume and the Fe mass in the outflow was estimated using the breakthrough curves in Figure 1c. The total mass of iron in the sand before and the injected GT-nZVI was higher compared to the Fe measured in the outflow and sand after the experiments for all four columns. The pure sand showed a deficit of 22 % on average and the Al-coated sand a deficit of 33 % on average. Even though these differences may be partially attributed to the error introduced by the used methods (the “missing” mass was very small), we did identify another sink for Fe that can account for the remaining mass and the difference between the two types of sands: the filters used in the exit of the columns showed accumulation of iron, with a characteristic red colour. The filters used had a nominal size of 0.7 μm, which indicates that particles larger than 700 nm would be retained by the filter. Visual observations confirmed that the amount of reddish-brown accumulated particles in the outflow of the Al-sand filter was higher compared to the pure sand filters. This indicates that enhanced agglomeration of particles in the Al-coated sand column caused greater retention by the filter, which can explain both the lower amount on the sand and the narrower breakthrough curve.

Aluminium hydroxide has an isoelectric point of approximately 9, which means that it is positively charged at pH values lower than 9 and it would have a strong positive charge in the pH range observed in this study. Silica, on the other hand, has very low negative charge throughout the pH spectrum, because of the weakly interacting Si-O bonds at the surface. Iron nanoparticles have an isoelectric point between 8 and 8.5, below which they also develop a positive charge (Sun et al., 2006). The interaction between the nanoparticles and the organic coatings will depend both on the pH and the nature of the coating. Most polyphenols have pKa values between 7 and 9 (Perron et al., 2008), which means that maximum deprotonation will occur above these values. Thus, increased particle aggregation should be favoured at pH below 7 because of compression of the electric double layer (Kim et al., 2012). However, polyphenol-coated nanoparticles should be positively charged at low pH, because polyphenols are increasingly neutral with decreasing pH. This in turn, indicates that the Al surfaces on the coated sands are likely to repel the nanoparticles, while silica surfaces are likely to attract them. This analysis is consistent with the observations in the columns, which showed no accumulation of Fe on the Al-coated sand, and some deposition on the pure silica sand.

4. Conclusions

The transport characteristics of iron nanoparticles prepared with green tea, polyphenol-rich solution, were investigated for two granular media, pure silica sand and sand coated with aluminium hydroxide. The GT-nZVI injection caused a sharp decrease in the effluent pH from 8.5 to 2, because of the residual free Fe^{3+} in the solution and the associated hydrolysis reactions. The redox potential increased from 150 mV to 550 mV, even though the GT-nZVI contains reducing Fe^0. This phenomenon is attributed to the oxidation of polyphenols that are present in green tea. The increase in redox potential may be used as an indicator of GT-nZVI transport in the subsurface when applied as in situ reactant.
The breakthrough curves for total Fe in the outflow indicated that some aggregation and deposition of nanoparticles occurred in the both types of sand, similar to other types of nZVI previously studied. However, the majority of the iron mass was obtained in the outflow (73 % in the uncoated and 62 % in the coated sand), indicating good transport characteristics for the nanoparticles. XRF results indicated that no iron was retained on the Al-coated sand particles, while 4 % of the injected Fe was deposited on the pure silica particles. This behaviour is attributed to the electrostatic interactions between the positively charged nanoparticles and the positively charged Al-coatings vs. negatively charged silica in the pH range of the experiments. The “missing” iron in the Al-coated sand columns was observed as a reddish brown precipitate in the 0.7 μm filter that was located in the outflow of the columns; thus, increased agglomeration was observed compared to the pure silica sand columns. This study shows that soil chemistry has an important effect on the transport of nanoparticles in porous media.

References

Cao J., Zhang W., 2006, Stabilization of chromium ore processing residue (COPR) with nanoscale iron particles, J. Haz. Mater. 132, 213-219.

Chen J., Truesdail S., Lu F., Zhan G., Belvin C., Koopman B., Farrah S., Shah D., 1998, Long term evaluation of aluminum hydroxide coated sand for removal of bacteria from wastewater, Wat. Res. 32, 2171-2179.

Chrysochoou M., Johnston C., Dahal G., 2012. A comparative evaluation of hexavalent chromium treatment in contaminated soil by calcium polysulfide and green-tea nanoscale zero-valent iron, J. Haz. Mater. 201-202, 33-42.

Elliott D., Zhang W., 2001, Field assessment of nanoparticles for groundwater treatment, Environ. Sci. Technol. 35, 4922–4926.

Franco D.V., Da Silva L.M., Jardim W.F., 2009, Reduction of Hexavalent Chromium in Soil and Ground Water Using Zero-Valent Iron Under Batch and Semi-Batch Conditions, Water Air Soil Poll. 197, 49-60.

Hoag G.E., Collins J.B., Holcomb J.L., Hoag J.R., Nadagouda M.N., Varma R.S., 2009, Degradation of bromothymol blue by ‘greener’ nano-scale zero-valent iron synthesized using tea polyphenols. J. Mater. Chem., 19, 8671-8677.

Kanel S.R., Choi H., 2007. Transport characteristics of surface-modified nanoscale zero-valent iron in porous media, Wat. Sci. Technol. 55, 157-162.

Kim H.-J., Phenrat T., Tilton R.D., Lowry G.V., 2012, Effect of Kaolinite, Silica Fines and pH on Transport of Polymer-modified Zero Valent Iron Nanoparticles in Heterogeneous Porous Media, J. Coll. Interf. Sci., in press, doi: 10.1016/j.jcis.2011.12.059.

Li X., Elliot D., Zhang W., 2006. Zero Valent Iron Nanoparticles for Abatement of Environmental Pollutants: Materials and Engineering Aspects, Crit. Rev. Solid State Mater. Sci., 31, 111-122.

Phenrat T., Kim H.-J., Fagerlund F., Illangasekar T., Tilton R.D., Lowry G.V., 2009. Particle Size Distribution, Concentration, and Magnetic Attraction Affect Transport of Polymer-Modified Fe^0 Nanoparticles in Sand Columns, Environ, Sci, Technol. 43, 5079–5085.

Perron N.R., Hodges J.N., Jenkins M., Brumaghim J.L., 2008, Predicting How Polyphenol Antioxidants Prevent DNA Damage by Binding to Iron, Inorg. Chem. 47, 6153-6161.

Reardon E.J., 2005, Zerovalent irons: styles of corrosion and inorganic control on hydrogen pressure buildup, Environ. Sci. Technol. 39, 7311-7317.

Sun Y.-P., Li X., Cao J., Zhang W., Wang H.P., 2006, Characterization of zero-valent iron nanoparticles, Adv. Coll. Interf. Sci. 120, 47-56.